

Model of the catalytic $A + B \rightarrow 0$ reaction with surface reconstruction

G. Zvejnicks and V. N. Kuzovkov

Institute for Solid State Physics, University of Latvia, Kengaraga 8, LV-1063 Riga, Latvia

(Received 27 February 2002; published 21 August 2002)

The $A + B \rightarrow 0$ reaction model with a surface reconstruction is analyzed. It is compared with another similar model for the $A + 1/2B_2 \rightarrow 0$ reaction [V. N. Kuzovkov *et al.*, J. Chem. Phys. **108**, 5571 (1998)], which mimics the CO oxidation reaction on the Pt surfaces. The effect of monomer B adsorption instead of dimer B_2 is examined. It is shown that qualitative system features such as reactant concentration oscillations are independent of this substitution.

DOI: 10.1103/PhysRevE.66.021109

PACS number(s): 82.20.Wt, 82.65.+r, 82.40.Np

I. INTRODUCTION

Detailed interpretation of catalytic surface processes is challenging for both practical applications and fundamental science. In particular, the heterogeneous catalytic surface reactions show a rich variety of behavior. For example, oxidation of CO or reduction of NO belong to a class of dissipative systems, which under certain conditions demonstrate a qualitatively new behavior on macroscopic length scales known as *spatiotemporal structures* (see, e.g., review paper [1]). It was shown there that it is surface reconstruction which plays an important role in the formation of such spatiotemporal structures.

One of the basic methods exploited to model the catalytic reaction systems is Monte Carlo (MC) computer simulations [2,3]. From the theoretical point of view, an application of the MC method to physical problems and to the heterogeneous catalytic reactions, in particular, is bounded only by the advances of computers. However, in reality the greatest large scale computer simulations of systems with fast diffusion [4,5] have considered linear sizes and diffusion, which are many orders of magnitude less than typical experimental ones. Due to this reason, the underlying theoretical models are as simple as possible and additional assumptions, such as neglect of some elementary steps (diffusion, desorption, or reconstruction), are quite common.

In this manner, a CO oxidation was modeled in the pioneering paper by Ziff, Gulari, and Barshad (ZGB) [6] as a monomer-dimer reaction $A + 1/2B_2 \rightarrow 0$, where several real processes were neglected (e.g., diffusion and reconstruction). We use here the traditional notations where $A = \text{CO}$ and $B_2 = \text{O}_2$, and the symbol 0 means that the product of reaction AB (CO_2) desorbs from the surface immediately after the reaction, leaving vacant sites. It is known that the ZGB model gives the second-order phase transition (B poisoning), which contradicts the experimental results. This stems from the assumption that a metal surface is assumed as a single square lattice where monomers and dimers are absorbed on the same lattice sites. A more refined model has to consider sublattices that correspond to the top, bottom, and bridge positions, thus describing the specific adsorption places for each type of atom. Such complicated models, e.g., CO + NO reaction [7], are very didactic but the realistic *scenario* of adsorption and reaction with a wide reactive window can be found only using MC. The realistic simulations have one

disadvantage: complicated models require a vast number of parameters, which limit their application exclusively to stationary processes.

The B -poisoning problem in the ZGB model becomes obsolete when one considers the *oscillatory reactions* driven by the surface reconstruction [4,5,8,9]. The point is that in the oscillatory regime, an oxygen (reactant B), as follows from simulations, never forms a dense layer. Therefore, models based on the ZGB scheme in this case are justified while sublattice models are not effective due to their extreme complexity. More so, it has been detected that reaction details weakly affect the kinetics. For example, the coordination number of a lattice changes in the course of reconstruction. However, it is almost impossible to simulate such topological effects [9]. It was suggested [10] that the reconstruction mechanism is independent of the coordination number. Then, the kinetics of the oscillatory processes (e.g., CO + NO reaction [5]) depends on the coordination number at high coverage of adsorbed particles when adsorption of dimers is hindered.

Before formulating the main goal of this paper, we would like to stress two important facts. First, as noted above, the B poisoning disappears in the oscillatory regime. Second, many free lattice sites are produced due to a fast diffusion of reactants A (CO) and following annihilation reaction with reactants B ($1/2\text{O}_2$). These two facts lead to the assumption that the natural condition for the O_2 dimer adsorption [the two empty nearest neighbor (NN) sites are required] is not so strict. Therefore, we can formulate the following hypothesis, which is proved in the present paper. *The geometrical aspect of a dimer adsorption into two lattice sites is not crucial for the observation of oscillating reactions with the surface reconstruction step.* In other words, a qualitatively similar kinetics should be achieved also for the monomer-monomer reaction, $A + B \rightarrow 0$. (The symbol 0 stays here as before for the product of reaction AB which desorbs from the surface immediately after reaction.) We would like to stress that the $A + B \rightarrow 0$ reaction has a wide area of applications beside the description of surface processes. In particular, for the Frenkel defects in the bulk [11–13] this reaction describes defect annihilation which restores the ideal crystalline structure. (In this case a symbol 0 literally stays for the absence of defects.)

At a first glance such a substitution is impossible since the qualitative behavior of the ZGB and $A + B \rightarrow 0$ models

strongly differs. To demonstrate this, let us denote the adsorption rates of reactants A and B with ζ and $1 - \zeta$, respectively. There is a reactive window in the original ZGB model when adsorption rates lie in the relatively wide region $0.395 < \zeta < 0.525$ [6]. On the other hand the nontrivial result is only possible in the $A + B \rightarrow 0$ reaction without desorption when both adsorption rates coincide, i.e., at the point $\zeta = 0.5$. For $\zeta < 0.5$ and $\zeta > 0.5$ values, the model gives B and A poisoning, respectively. The considered differences are legitimate without surface reconstruction. However, when one takes into account that each type of atom and molecule adsorbs differently on reconstructed and nonreconstructed surfaces (due to different sticking coefficients), and that the two-phase systems are dynamical, then our previous statement makes sense. Nevertheless, it has to be proved by MC simulations.

The mentioned substitution of reactions was also used in the past. So, Hildebrand *et al.* [14] have considered the so-called hypothetical model system where diffusion, adsorption, and desorption characteristics of the reactants A and B correspond to CO and O in a CO oxidation reaction, respectively, but the annihilation reaction is $A + B \rightarrow 0$. In this case the surface reconstruction step was ignored but the reactive window was achieved by introducing two different sets of adsorbing sites for A and B , and desorption of one type of reactant. The reaction was treated using so-called mathematical modeling, i.e., the mean-field approximation, which has no large precision in describing reactive systems [2,11,12].

One of the simplest bimolecular reactions, $A + B \rightarrow 0$, has attracted attention already for a long time (see review papers [11–13,15]). In the pioneering analytical paper by Ovchinnikov and Zeldovich [16] for the first time it was suggested that the kinetic law of mass action is violated. As a consequence, the standard chemical kinetics was shown to be incorrect at asymptotically long time. For example, for the $A + B \rightarrow 0$ reaction with equal concentrations of both reactants, $C_A = C_B = C$, the standard kinetics predicts that the concentration decay $C \propto t^{-1}$, as $t \rightarrow \infty$. However, it was shown [11–13,15,16] that this prediction corresponds to the mean-field approximation and it is true only for high-dimensional systems, $D \geq D_0 = 4$. In the low-dimensional systems $D < D_0$ with diffusion controlled processes, the nonstandard kinetics occurs, $C \propto t^{-D/4}$. Several years later this was proved by Toussaint and Wilczek [17] using the MC simulations. Thus, the role of computer modeling was demonstrated as a tool for evaluating new ideas on which the microscopical models were based.

The vast amount of literature on $A + B \rightarrow 0$ reaction can be divided into two groups. First, it is relaxation kinetics without the reactant source, [11,12,15]. Second, the kinetics of reactant accumulation and corresponding concentration saturation (if it exists) with a permanent particle source [11,12,15,18,19]. The latter is naturally related to the topic discussed here.

Several modifications of the $A + B \rightarrow 0$ model with a particle source have been studied. Desorption of one type of reactant [20] eliminates the poisoned state for different A - and B -adsorption rates. To model the surface disorder, two types of surface sites with different adsorption rates have

been distributed randomly in the system by Frachenbourg *et al.* [21]. It is shown that the disorder leads to the reactive state. In a similar way two distinct types of sites for each adsorbant with different adsorption coefficients are used to analyze an optimal structure of a bimetallic catalyst [22], where, contrary to the previous paper, both types of sites form a periodic structure.

To prove the idea given above, we extend the two-dimensional $A + B \rightarrow 0$ model to the case of surface reconstruction: two surface states with different adsorption rates for each reactant are introduced. Contrary to the static distribution of various adsorption sites [21,22], the type of sites can change in time as a surface reconstruction step [4,8,10,23]. The limit of a fast reactant diffusion is considered.

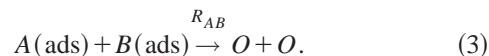
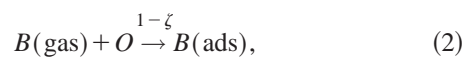
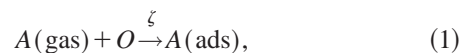
The paper is organized in the following way. The generalized $A + B \rightarrow 0$ model is introduced in Sec. II. Sections III and IV present results of MC computer simulations and their analysis, respectively. General conclusions are given in Sec. V.

II. MATHEMATICAL MODEL

The application of the MC method assumes use of a mathematical model which contains the definitions of reactants (atoms, molecules, etc.) and basic reactions between these reactants (adsorption, desorption, reaction, etc.). The corresponding *transition rates* used in MC simulations are obtained by means of the master equation [24].

The standard rules for the simplest monomer-monomer annihilation reaction, $A + B \rightarrow 0$, are as follows.

(i) Adsorption of reactants A (B) from a gas phase onto empty sites O with independent rates p_A and p_B , respectively. For simplicity, we assume that time is measured in units of $1/p$, where $p = p_A + p_B$. Thus in the new unit system, adsorption rates of reactants A and B are normalized to unity, Eqs. (1) and (2), respectively,



(ii) Annihilation reaction, Eq. (3), between reactants A and B takes place with the rate R_{AB} only for a pair of NNs A and B .

The complementary rules are adapted from the ZGB model with the surface reconstruction [4,5,8,10,23]. Thus, the $A + B \rightarrow 0$ model is used as a simplified description of the CO catalytic oxidation on Pt surfaces, where reactants A stay for CO molecules and B for O atoms.

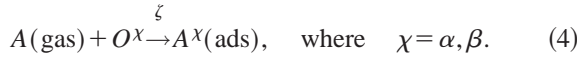
It is detected experimentally that the following processes are significant for the CO catalytic oxidation reaction. First, the diffusion of CO molecules is known to be a fast and important process, which can lead to the formation of spatiotemporal structures [1]. Second, it is the surface reconstruction which is a driving force of oscillatory behavior. It is

shown that in the absence of adsorbates the *reconstructed* surfaces of Pt(100) and Pt(110) are stable [1]. On such reconstructed surfaces, adsorption of oxygen is hindered. Adsorbed CO molecules are known to change the surface energy, which results in surface backward reconstruction (nonreconstructed state) which takes place above some critical CO adsorbate concentration. It is known that O_2 adsorption on nonreconstructed surfaces is effective. In this regime the CO oxidation takes place. When the amount of CO drops below critical, the surface reconstruction takes place and adsorption of O_2 becomes hindered. Let us generalize the standard model to include these effects.

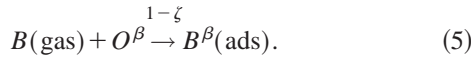
A. Reconstructed and nonreconstructed phases

Two different surfaces (phases), denoted hereafter as α and β , are introduced. (α is the reconstructed and β is the nonreconstructed phase.) This allows both (i) processes (such as adsorption, diffusion) to proceed differently in each phase, and (ii) to implement the surface reconstruction mechanism, which transforms one phase into another.

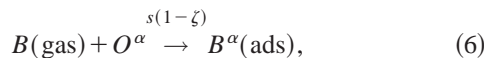
Keeping in mind the experimentally detected differences between CO and O_2 adsorption, it is assumed that adsorption of reactants A and B proceeds differently in each phase. Adsorption of reactants A (CO) is allowed in all empty lattice sites irrespective of the phase, Eq. (1), which is valid for both α and β phases,



In contrast, the adsorption of reactants B (O_2) with the probability $1 - \zeta$, Eq. (2), is allowed only in the β phase,



Adsorption of B in the α phase is determined by the reaction



where the sticking coefficient s is chosen in the interval between 0 and 1. The limiting case of $s=0$ corresponds to reactant B adsorption exclusively in the β phase. In its turn, the opposite limit $s=1$ leads to uniform reactant B adsorption on the lattice, irrespective of phase.

The different values of parameter s mimic different crystallographic orientations of a crystal. To this end, let us consider the O_2 adsorption on the Pt surface as an example. On the Pt(100) surface the ratio of O_2 adsorption on nonreconstructed (β phase) vs reconstructed phases (α phase) is $\sim 10^{-3}$, while on Pt(110) this ratio is ≈ 1 [1]. It means that there is practically no O_2 (B) adsorption on the Pt(100) reconstructed surface ($s=0$), while on the Pt(110) surface O_2 can be adsorbed on the reconstructed surface ($s>0$).

B. Surface reconstruction

It is known that the surface reconstruction mechanism on Pt monocrystals is associated with adsorbed CO molecules

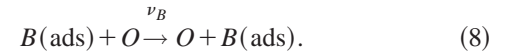
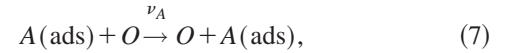
[1]. Therefore, the following reconstruction model was proposed [23]: Let us assume the phase boundary, i.e., two NN sites which are in a state $\alpha\beta$. If reactant A (CO) is present on one of these sites, it induces the α phase growth with the rate V . The eventual surface state then reads as $\alpha\alpha$. When there are no reactants A on the phase boundary, the β phase grows with the rate V . In this case the eventual state is $\beta\beta$.

C. Nucleation

The model also allows extension for the case of spontaneous phase nucleation. It is assumed that a single-surface site, which is initially in a phase α or β , can change its phase spontaneously to β or α [10], respectively. This process is independent of the phase of the neighboring sites and type of reactant adsorbed on the site. The process is modeled as a weak noise, which produces phase defects. Its rate γ is by several orders of magnitude less than rates of other processes.

D. Diffusion on a single phase

Diffusion of both reactants A and B is assumed as jumps to the NN empty sites with the jump rate ν_A and ν_B , respectively,



Hereafter we distinguish the *symmetric* diffusion case when both rates in Eqs. (7) and (8) coincide ($\nu_A = \nu_B$), and *asymmetric* diffusion when these rates are different ($\nu_A \neq \nu_B$).

E. Diffusion over a phase boundary

Besides the reactant adsorption, the reactant diffusion depends on the phase properties as well. Experimentally detected different reactant concentrations in different phases [1,25–28] can be explained by the membrane effect [10,29]: Reactant jumps from α to β phase are promoted, while the reverse jumps are suppressed. This results in reactant accumulation in the β phase. To describe the membrane effect, let us define the *boundary jump rate* κ as follows:

$$\nu_{\alpha\beta} = \nu(1 + \kappa), \quad (9)$$

$$\nu_{\beta\alpha} = \nu(1 - \kappa), \quad (10)$$

where $\nu_{\alpha\beta}$ and $\nu_{\beta\alpha}$ are jump rates from α to β and vice versa, respectively. Asymmetry in the jump rates, Eqs. (9) and (10), is directly connected with the membrane effect. Mathematically the parameter κ varies in the interval $[-1,1]$, while the physically interesting case is $[0,1]$. The physical basis for asymmetric diffusion is a higher CO adsorption energy on the β phase [25,26], which leads to promoted CO diffusion from the α to β phase.

One can express the boundary jump rate from Eqs. (9) and (10) as a dimensionless parameter,

$$\kappa = \frac{\nu_{\alpha\beta^-} - \nu_{\beta\alpha}}{\nu_{\alpha\beta^+} + \nu_{\beta\alpha}}. \quad (11)$$

Hereafter, we call the case $\kappa > 0$ *membrane diffusion*.

III. MONTE CARLO RESULTS FOR THE GENERALIZED $A+B \rightarrow 0$ MODEL

The MC computer simulations are based on the algorithm that was explained in details in [24]. Results of simulations are analyzed with the *power spectral density* (PSD) method, [24] which gives us the amplitude and frequency of oscillations. The time unit is proportional to one Monte Carlo step, i.e., when each lattice site is considered on average at least one time. The proportionality coefficient depends on the rates of elementary processes [24]. Time units are omitted when describing rates and simulation time, since their product is dimensionless and we consider the theoretical model. For example, when inverse rates are measured in seconds, the time unit is also a second.

Any reactant desorption is neglected. It was shown [8] that the oscillation mechanism on Pt(110) is governed by both factors: strong O_2 adsorption on the reconstructed phase (large s values) and reactant A desorption which eliminates the A -poisoning effect. However, in the case of Pt(100) the oscillation mechanism is different and the neglect of reactant A desorption has no decisive role. By this reason, our neglect of desorption means that the obtained results can be compared only with results [8] discussing local oscillations observed on Pt(100) surfaces.

Similarly, the role of the membrane effect ($\kappa > 0$) in the oscillatory reactions has to be considered from the point of view of physics on the same Pt(100), since the membrane effect is important for this surface [10,29].

A. The standard model with surface reconstruction

Let us consider the limiting case of asymmetric diffusion with mobile reactants A and immobile B . We neglect the membrane effect ($\kappa = 0$), i.e., the diffusion of A over the $\alpha\beta$ phase boundaries is symmetric, irrespective of the phase type from which the boundary is approached. The phase reconstruction is allowed. The following dimensionless parameters are chosen: $\nu_A = 100$, $R_{AB} = 100$, and $V = 1$. As it was shown in the limit of constant reactant A coverage [23], the β phase is stable and it has reached a saturation for these parameters. The default lattice size L is chosen to be $L = 256$ lattice sites if not explicitly stated differently. Figure 1 shows concentration oscillations for three different ζ values. Oscillatory behavior, in general, is irregular and it proceeds as pulses, which are characterized by the change of oscillation amplitude in time. The oscillation amplitude and frequency depend on the adsorption rate ζ . The pulse-type behavior detected in MC simulations is similar to the experimentally observed pattern of reactant concentration oscillations on Pt(100) [30,31].

The origin of oscillations has a simple explanation. Let us start at the instant when A 's concentration has a maximum. At this stage reactants A ensure an increase of the β phase.

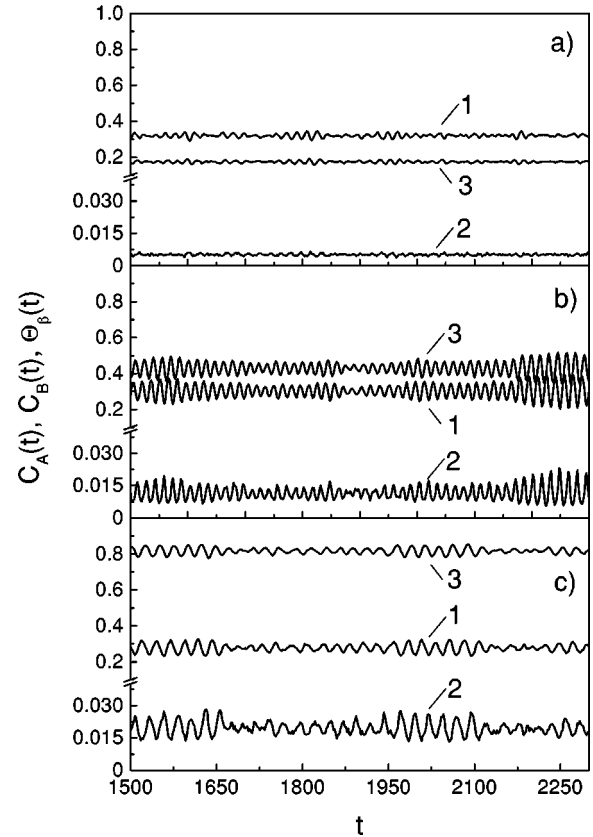


FIG. 1. Temporal evolution of concentrations: reactants A (1), B (2), and β phase (3). Adsorption rate ζ is 0.15 (a), 0.30 (b), and 0.45 (c).

The β phase allows to adsorb additional B reactants. The reaction between A and B effectively decreases the amount of A in the considered region. The concentrations of A and B reach the minimum and maximum, respectively. The β phase becomes unstable without A and its concentration reaches a minimum. The amount of β phase has been depleted in the same area where it is in excess. In this region reactants A are adsorbed intensively, but not B . One can think of these processes as *waves of concentrations*.

Let us now analyze the system qualitatively. It is readily seen from Fig. 2 that the mean concentrations reveal *two* qualitatively different types of behavior depending on the reactant A -adsorption rate ζ . To avoid the finite-lattice size effects, a spontaneous phase nucleation is included whenever necessary in the model, see corresponding notes under figures and explanations in the Appendix.

(i) The first region is characterized by the nonzero AB production \mathcal{R}_{AB} . Concentration oscillations are detected, whose amplitudes depend on both reactant A creation rate ζ and lattice size L . First, let us look at the case of oscillation dependence on ζ for the fixed lattice size $L = 256$. The MC simulations show that there exists a frequency maximum at $\zeta = 0.3$ and an oscillation amplitude maximum at $\zeta = 0.375$, see Fig. 3(a). However, these ζ values do not coincide.

An inclusion of reactant B diffusion brings no qualitatively new effects to the oscillatory behavior as compared with immobile B . The frequency of oscillations increases but

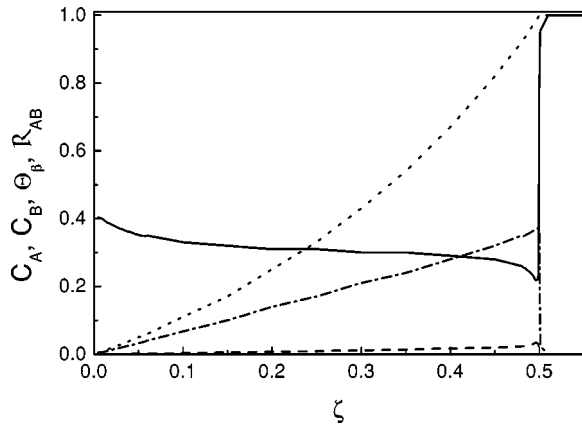


FIG. 2. Mean concentration of reactants A (solid line), reactants B (long dashed), β phase (short dashed), and AB production \mathcal{R}_{AB} (mixed long and short dashed) vs the adsorption rate. The spontaneous phase creation $\gamma = 10^{-4}$. Parameters used: $\nu_A = 100$, $\nu_B = 0$, and $R_{AB} = 100$.

only slightly, Fig. 3(b). An increase of oscillation amplitude is better pronounced but shows qualitatively the same dependence on ζ as in the limit of immobile B , Fig. 3(b).

Second, the oscillation amplitude depends on the lattice size. In order to show this dependence, the signal-to-noise ratio (SNR) [32–39] is exploited. SNR was used there for detecting the stochastic resonance phenomena [40], which was defined as an amplification of the output signal with an increase of the noise level.

Here we adapt the SNR definition as the ratio of the PSD peak at the system's oscillation frequency to the average am-

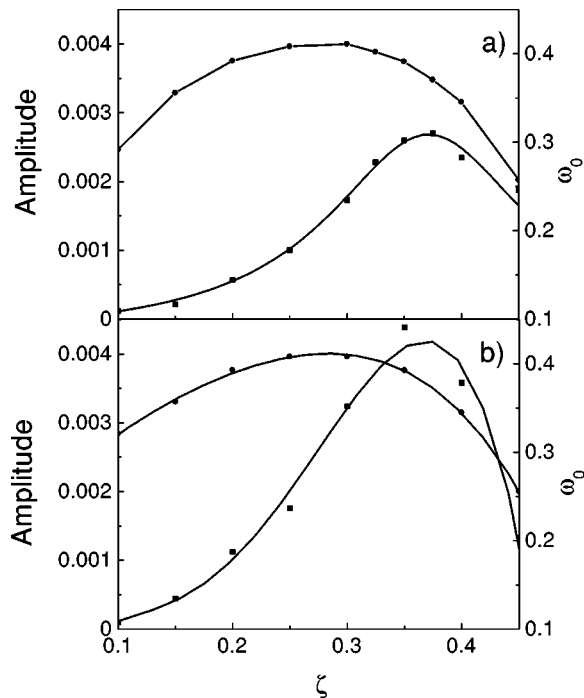


FIG. 3. Amplitude (squares) and frequency (circles) dependence on the creation rate ζ of reactants A . Parameters: asymmetric diffusion $\nu_A = 100$, $\nu_B = 0$ (a) and symmetric diffusion $\nu_A = \nu_B = 100$ (b).

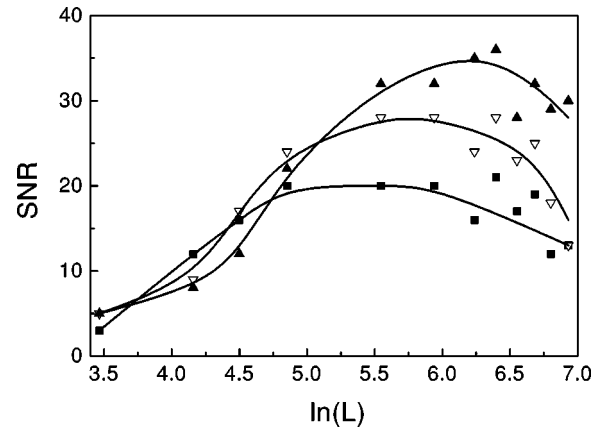


FIG. 4. The SNR dependence on the linear lattice size. The jump rate ν_A is 100 (squares), 150 (down triangles), and 200 (up triangles). Parameters $\zeta = 0.35$, $\nu_B = 0$.

plitude of the background noise level in the vicinity of the PSD peak [38]. The SNR has a maximum for certain lattice sizes, Fig. 4 (note the logarithmic scale), depending on the jump rate. It indicates that the nature of observed oscillations is the stochastic resonance. An amplitude of oscillations, which is proportional to PSD, plays the role of a signal and decreases with the lattice size. The noise level decreases with the size of the lattice as well. In its turn, the SNR, which is the ratio of the above-mentioned values, increases for certain noise and signal combinations, which is characteristic for the stochastic resonance. More so, it is detected that diffusion plays the role of the synchronization mechanism of oscillations in the stochastic resonance, see Fig. 4. Larger jump rates result in both the SNR increase and synchronization of oscillations for larger lattice sizes.

The dispersion of the results in Fig. 4 are due to a pulse-type behavior of oscillations, see Fig. 1. For the same dataset the pulses can produce slightly different PSD values depending on the data interval which is used in the PSD calculations (e.g., a whole pulse is included or only its half).

(ii) The second region can be classified as the reactant A -poisoned β phase. It is observed for the adsorption rates that $\zeta \geq 0.5$. The transition to the uniform β phase occurs gradually. First, adsorbed reactants A promote the formation of β phase, while the α phase is eliminated completely. The nucleation plays almost no role, since it is too weak to make the impact on a macroscopic behavior. It only smoothes transition from region (i) to (ii) around the point $\zeta = 0.5$, see Fig. 2. This situation corresponds to the adsorption of reactants A and B uniformly on a whole lattice. Since the A -adsorption rate is greater than that of B , it is only a question of time when the system arrives at the A -poisoned state.

B. Membrane effect

Let us assume now the asymmetric membrane diffusion of reactants A with immobile B . For example, for $\kappa > 0$, jumps from the α to β phase are promoted while reverse jumps are hindered. In other words, the β phase acts as an effective trap of A reactants. Once reactants A find themselves in the β phase, they jump with the same rate as be-

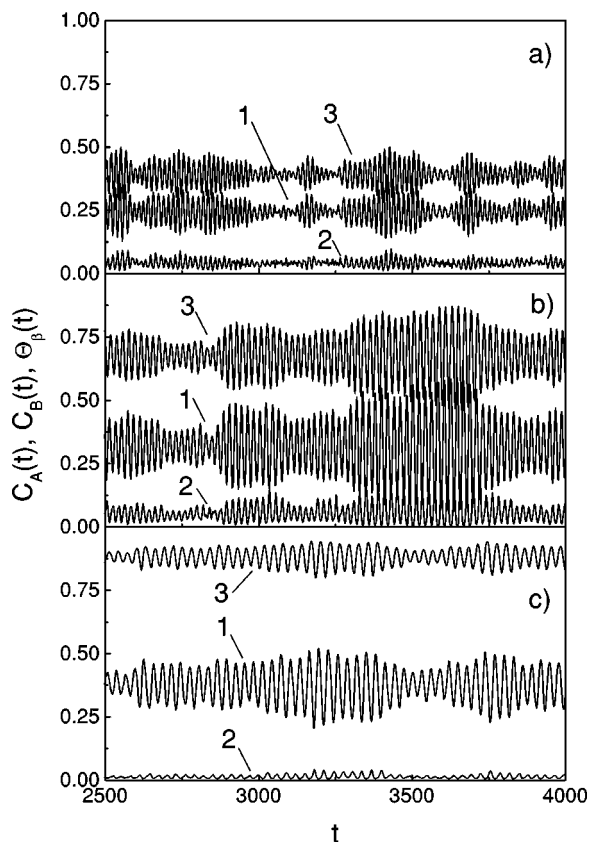


FIG. 5. Temporal evolution of concentrations in the reactant A membrane diffusion case: reactants A (1), B (2), and β phase (3). The $\zeta=0.20$ (a), $\zeta=0.35$ (b), and $\zeta=0.45$ (c) figures. Parameters: $\nu_A=100$ and $\kappa=0.9$.

fore. The only difference is that now A diffusion is restricted by the size of the β phase and the height of the activation barrier, when reactants A try to leave the β phase. As an example, let us consider the limit of the strong membrane effect, $\kappa=0.9$. It was shown [8,29] that the chosen κ value approximately describes the properties of Pt(100) surfaces, since it leads with a good precision to both critical values of A concentrations necessary to maintain homogeneous surface phases.

In general, oscillation amplitudes increase with the reactant A membrane diffusion, see Fig. 5. The quasiperiodic oscillatory behavior is also amplified, in comparison with the nonmembrane diffusion case, Fig. 1. It is evident in Fig. 5 that oscillations proceed as pulses with a different lifetime.

The interpretation of the origin of these oscillations is similar to the case of $\kappa=0$. The maximum amount of reactants A promotes the growth of the β phase. When the β phase reaches its maximum, it results in two effects: First, it traps A and they are bound by the β phase. Second, reactants B are intensively adsorbed on the β phase. A reaction between A and B results in a decrease of A concentration while B reactants are continuously adsorbed. It leads to an excess of B's, which have no A partners for the reaction.

The minimum of A concentration leads to the collapse of the β phase. At this stage reactants A are adsorbed but B adsorption is minimal. The reactants B, which were accumu-

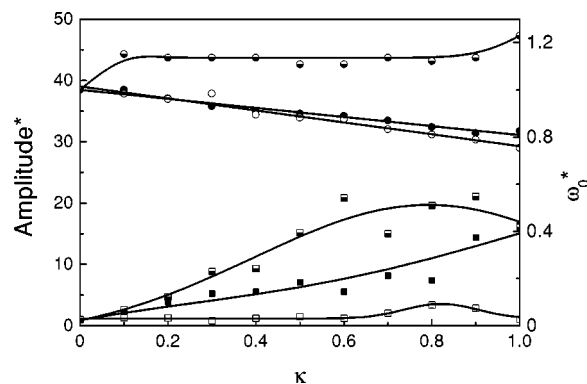


FIG. 6. The relative amplitude (squares) and frequency (circles) dependence on the membrane diffusion. Values are normalized to the nonmembrane diffusion case ($\kappa=0$). The $\zeta=0.20$ (half filled), $\zeta=0.35$ (filled), and $\zeta=0.45$ (open) symbols. Parameter $\nu_A=100$.

lated during the maximum of the β phase, readily react with adsorbing A. Thus, the concentration of B decreases, but that of A increases. Reactants A create new β phases everywhere except in those regions where it already was created. The β phase is created in local regions asynchronously, due to a finite rate of reactant A diffusion.

The trapping of reactants A obviously makes the β phase more stable and promotes the oscillatory behavior, see Fig. 6. The dispersion of results comes from the pulse-type oscillations, see Fig. 5.

The membrane diffusion reveals three main results. First, the strong oscillation amplitude increase is observed (with respect to the nonmembrane diffusion case, $\kappa=0$) for $\zeta=0.20$. Oscillations frequency remains constant in the interval $0.1 \leq \kappa \leq 0.9$, while for the limiting κ values 0 and 1 the frequency slightly decreases and increases, respectively. Second, the oscillation amplitude increases with the boundary jump rate at $\zeta=0.35$. Its increase has a maximum for $\kappa=1$, i.e., reactants A once trapped by the β phase stay there forever. Third, the oscillation amplitude remains constant for $\zeta=0.45$ until $\kappa < 0.8$. It means that the high concentration of reactants A and their trapping into the β phase do not affect the oscillatory behavior. In this regime an increase of κ up to unity leads to the stationary state, when the β phase covers a whole lattice and thus there is no chance for the α phase to develop. No oscillatory behavior is possible in this case. To overcome the problem of the β poisoning, the point at $\zeta=0.45$ and $\kappa=1$ in Fig. 6 is calculated with spontaneous phase creation $\gamma=10^{-5}$. In this case a decrease of oscillation amplitude is observed. The oscillation frequency decreases linearly with κ , but with different slopes for the last two cases. The larger the ζ is, the steeper is the slope. The decrease of frequency indicates that the period between two successive maximums of concentration increases due to the time needed for promoted lattice reconstruction.

C. Reactant B adsorption on α phase

As the next limiting case, let us consider the adsorption of reactants B on the α phase, i.e., the nonzero s values. In the limiting case of $s=1$ the reconstruction has no effect and the

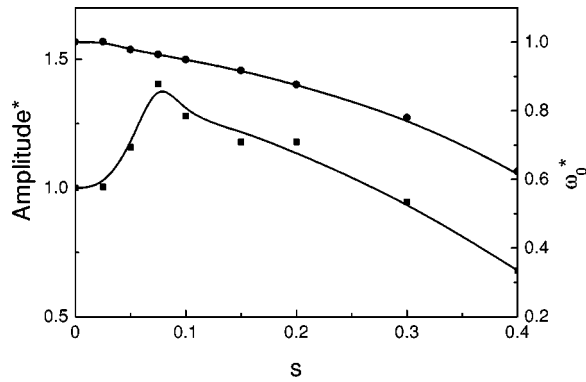


FIG. 7. The relative amplitude (squares) and frequency (circles) dependence on B -adsorption rate on the α phase s . Values are normalized to the $s=0$ case. Parameters: $\zeta=0.35$, $\nu_A=100$, $V=1$, and $R=100$.

model coincides with the standard $A + B \rightarrow 0$ annihilation reaction. It is known that the latter reveals the B and A poisoning for $\zeta < 0.5$ and $\zeta > 0.5$, respectively. Only at the point $\zeta = 0.5$, when both types of reactants are created with absolutely equal probability, the system shows the reaction regime. MC simulations show that poisoning states are reached already for $s < 1$. First, an increase of s slightly increases the oscillation amplitude, see Fig. 7. However, then the amplitude decreases while the B poisoning is reached, e.g., for $\zeta = 0.35$, the poisoning starts at $s > 0.4$. The frequency only decreases as s increases.

D. Examples of membrane diffusion and B adsorption

Let us fix the boundary jump rate at $\kappa=0.95$ and vary the adsorption rate ζ , see Fig. 8(a). The β phase serves now as a trap of A reactants. The oscillatory behavior is pronounced at $\zeta=0.35$, which is similar to the nonmembrane diffusion case, Fig. 3(a). The difference lies in the amplitude of oscillations, which increases almost by an order of magnitude in the membrane diffusion case. The membrane effect stabilizes the oscillations for small ζ values, e.g., the oscillations with $\kappa=0.95$ are observed for $\zeta \geq 0.04$, while in the nonmembrane case the poisoning occurred at $\zeta \leq 0.05$. The oscillation frequency depends also on ζ . Unlike the nonmembrane case, the frequency maximum is shifted to the lower values, $\zeta = 0.20$, instead of $\zeta = 0.30$. Comparing the values of frequencies in Figs. 3(a) and 8(a), one can see that membrane diffusion has almost no effect on the oscillation frequency at $\zeta \approx 0.20$. It is the marginal state which divides the two regions: (a) frequency increases for smaller ζ , see, e.g., $\zeta = 0.15$ case in Fig. 6, and (b) frequency linearly decreases for the larger ζ values.

As an example the limiting case with $s=0.1$ is studied for various ζ in Fig. 8(b). The amplitude is slightly increased in the region of the maximum (ζ varies in the interval 0.350–0.425), while the frequency is slightly decreased, in a comparison with no B adsorption on the α phase, see Fig. 3(a). The B poisoning occurs at the adsorption rates of $\zeta < 0.15$.

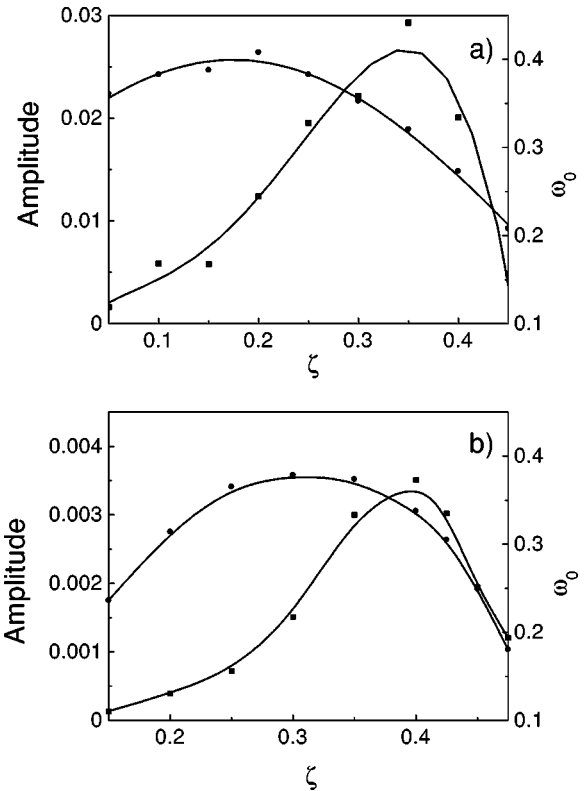


FIG. 8. The amplitude (squares) and frequency (circles) dependence on the adsorption rate ζ . Parameters: $\nu_A=100$, $V=1$, and $R=100$. Membrane diffusion $\kappa=0.95$ (a). B -adsorption parameter $s=0.1$ (b).

IV. CONCLUSIONS

The ZGB model of the $A + 1/2B_2 \rightarrow 0$ reaction with surface reconstruction is known to describe adequately the catalytic CO_2 formation on the Pt(110) and Pt(100) surfaces [4,8,10,23]. In the present paper the ZGB model was reduced to the $A + B \rightarrow 0$ model with surface reconstruction. The MC computer simulations show a *local* oscillatory behavior, which is not synchronized over the whole lattice. The oscillation amplitude and frequency depend on the reactant adsorption rate.

Several physically interesting limiting cases were studied. First, the reactant membrane diffusion over a phase boundary is considered. The amplitude of oscillations increases, if the diffusion of A 's over a phase boundary is promoted towards the β phase. In this case the β phase serves, in fact, as a trap for reactants A .

Second, in analogy with the Pt(110) surface, where B adsorption takes place on the α phase, we considered the hypothetical case when reactants B are adsorbed on the α phase. For small B -adsorption rate values on the α surface ($s \leq 0.1$) the oscillatory behavior is promoted, while larger B -adsorption rate values ($s > 0.1$) suppress oscillations. Oscillatory behavior in general is unstable. It manifests itself as quasiperiodic pulses of different lengths when the oscillation amplitude is determined by the size of lattice, i.e., we observe local oscillations.

It was shown [8] that the strong oscillatory behavior

arises as the consequence of both finite values of parameter s and desorption of reactants A (the condition for oscillations on Pt(110) [8] is $s \approx 0.5$, $k_A \sim 0.1$, desorption of A). We considered no A desorption in the present paper, therefore in a comparison with [8], we model a different oscillatory mechanism which is characteristic for the Pt(100) surfaces.

In conclusion, the generalized $A + B \rightarrow 0$ model with surface reconstruction predicts an increase of oscillatory behavior in the limit of reactant membrane diffusion and B creation on the α phase (e.g., $s = 0.1$). Oscillatory behavior is pulse type, which is in agreement with experimental studies of CO catalysis on Pt(100) surfaces [30,31]. These facts lead us to the conclusion that the $A + B \rightarrow 0$ model with surface reconstruction has qualitatively the same properties as the ZGB model with surface reconstruction [4,5,8,10,23]. Thus we have proven the hypothesis developed in Introduction.

V. GENERAL CONCLUSIONS

The real catalytic surface reactions usually reveal a very complex behavior which is characterized by a formation of the spatiotemporal structures. The theoretical description of reactions involves a number of elementary reaction steps. The simultaneous analysis of all reaction steps is as much complicated as the interpretation of experiment. Therefore, of our particular interest are simplified reaction schemes, focused on a study of the origin of spatiotemporal structures.

In the present paper the $A + B \rightarrow 0$ model was shown to have qualitatively the same behavior as the $A + 1/2B_2 \rightarrow 0$ model. The conclusion was drawn that the dimer (O_2) adsorption in the ZGB model is important for physical interpretation, but it gives no significant contribution to the understanding of the origin of oscillatory behavior. The peculiarities of the oscillatory behavior are caused by other

factors, e.g., the adsorption rate, asymmetric diffusion, and different adsorption probabilities on both reconstructed and nonreconstructed phases.

ACKNOWLEDGMENTS

The authors are thankful to E. A. Kotomin for fruitful discussions. Financial support from the European Center of Excellence in Advanced Materials Research and Technology (Contract No. ICA-1-CT-2000-7007) is appreciated.

APPENDIX: SURFACE POISONING

Let us analyze the reasons of surface poisoning. The main problem lies in the fact that once one of the existing phases α or β is eliminated completely, it cannot be created again. Development of any phase needs its seed, but it can happen that such a seed is no longer present in the lattice. This is a finite-lattice size effect since for infinite lattices such a seed should exist. For instance, for the adsorption rate $\zeta = 0.05$ the α phase poisoning, which occurs for lattices of size $L = 256$, changes for a reactive regime when both phases co-exist as $L = 1024$. Similarly, for $\zeta = 0.482$ the β phase poisoning occurs for the lattices of size $L = 256$, but an increase of the size up to $L = 4048$ brings the system into the reactive regime. In other words, an increase of lattice size extends the borders of the reactive region. However, it greatly increases the computational time as well. An effective way to overcome this finite-lattice size effect is to introduce a spontaneous transition reaction from one phase to another with a very small rate, say $\gamma = 10^{-5}$. This reaction was included in our model in the reactive region, in order to determine its impact on the system's behavior, but no substantial changes were found.

-
- [1] R. Imbihl and G. Ertl, *Chem. Rev.* **95**, 697 (1995).
 [2] E.V. Albano, *Surface Science*, Computational Methods in Surface and Colloid Science Vol. 89 (Dekker, New York, 2000).
 [3] E.V. Albano, *Heterog. Chem. Rev.* **3**, 389 (1996).
 [4] O. Kortlüke, V.N. Kuzovkov, and W. von Niessen, *Phys. Rev. Lett.* **83**, 3089 (1999).
 [5] O. Kortlüke, V.N. Kuzovkov, and W. von Niessen, *Phys. Rev. Lett.* **81**, 2164 (1998).
 [6] R.M. Ziff, E. Gulari, and Y. Barshad, *Phys. Rev. Lett.* **56**, 2553 (1986).
 [7] O. Kortlüke and W. von Niessen, *Surf. Sci.* **401**, 185 (1998).
 [8] V.N. Kuzovkov, O. Kortlüke, and W. von Niessen, *J. Chem. Phys.* **108**, 5571 (1998).
 [9] R.J. Gelten, A.P.J. Jansen, R.A. van Santen, J.J. Lukkien, J.P.L. Segers, and P.A.J. Hilbers, *J. Chem. Phys.* **108**, 5921 (1998).
 [10] V.N. Kuzovkov, O. Kortlüke, and W. von Niessen, *Phys. Rev. Lett.* **83**, 1636 (1999).
 [11] E. Kotomin and V. Kuzovkov, *Rep. Prog. Phys.* **55**, 2079 (1992).
 [12] E.A. Kotomin and V.N. Kuzovkov, *Modern Aspects of Diffusion-Controlled Reactions: Cooperative Phenomena in Bimolecular Processes*, Comprehensive Chemical Kinetics Vol. 34 (Elsevier, Amsterdam 1996).
 [13] V. Kuzovkov and E. Kotomin, *Rep. Prog. Phys.* **51**, 1479 (1988).
 [14] M. Hildebrand, A.S. Mikhailov, and G. Ertl, *Phys. Rev. Lett.* **81**, 2602 (1998).
 [15] P. Argyrakis, S.F. Burlatsky, E. Clement, and G. Oshanin, *Phys. Rev. E* **63**, 021110 (2001).
 [16] A.A. Ovchinnikov and Ya. B. Zeldovich, *Chem. Phys.* **28**, 215 (1978).
 [17] D. Toussaint and F. Wilczek, *J. Chem. Phys.* **78**, 2642 (1983).
 [18] L.W. Anacker and R. Kopelman, *Phys. Rev. Lett.* **58**, 289 (1987).
 [19] K. Lindenberg, B.J. West, and R. Kopelman, *Phys. Rev. Lett.* **60**, 1777 (1988).
 [20] E.V. Albano, *Phys. Rev. Lett.* **69**, 656 (1992).
 [21] L. Frachenbourg, P.L. Krapivsky, and S. Redner, *Phys. Rev. Lett.* **75**, 2891 (1995).
 [22] A.P.J. Jansen and C.G.M. Hermese, *Phys. Rev. Lett.* **83**, 3673 (1999).
 [23] O. Kortlüke, V.N. Kuzovkov, and W. von Niessen, *J. Chem. Phys.* **110**, 11 523 (1999).

- [24] G. Zvejniece and V.N. Kuzovkov, Phys. Rev. E **63**, 051104 (2001).
- [25] A. Hopkinson, J.M. Bradley, X.-C. Guo, and D.A. King, Phys. Rev. Lett. **71**, 1597 (1993).
- [26] A. Hopkinson, X.-C. Guo, J.M. Bradley, and D.A. King, J. Chem. Phys. **99**, 8262 (1993).
- [27] R.J. Behm, P.A. Thiel, P.R. Norton, and G. Ertl, J. Chem. Phys. **78**, 7437 (1983).
- [28] P.A. Thiel, R.J. Behm, P.R. Norton, and G. Ertl, J. Chem. Phys. **78**, 7448 (1983).
- [29] V.N. Kuzovkov, O. Kortlüke, and W. von Niessen, Phys. Rev. E **63**, 023101 (2001).
- [30] M. Eiswirth, P. Möller, K. Wetzl, R. Imbihl, and G. Ertl, J. Chem. Phys. **90**, 510 (1989).
- [31] R. Imbihl, M.P. Cox, and G. Ertl, J. Chem. Phys. **84**, 3519 (1986).
- [32] B. McNamara, K. Wiesenfeld, and R. Roy, Phys. Rev. Lett. **60**, 2626 (1988).
- [33] G. Debnath, T. Zhou, and F. Moss, Phys. Rev. A **39**, 4323 (1989).
- [34] L. Gammitoni, F. Marchesoni, E. Menichella-Saetta, and S. Santucci, Phys. Rev. Lett. **62**, 349 (1989).
- [35] G. Vemuri and R. Roy, Phys. Rev. A **39**, 4668 (1989).
- [36] T. Zhou, F. Moss, and P. Jung, Phys. Rev. A **42**, 3161 (1990).
- [37] D. Gong, G.R. Qin, G. Hu, and X.D. Weng, Phys. Lett. A **159**, 147 (1991).
- [38] D. Gong, G. Hu, X. Wen, C. Yang, G. Qin, R. Li, and D. Ding, Phys. Rev. A **46**, 3243 (1992).
- [39] D. Gong, G. Hu, X. Wen, C. Yang, G. Qin, R. Li, and D. Ding, Phys. Rev. E **48**, 4862(E) (1993).
- [40] L. Gammitoni, P. Hanggi, P. Jung, and F. Marchesoni, Rev. Mod. Phys. **70**, 223 (1998).